



Investigation of the tumoricidal effects of sonodynamic therapy in malignant glioblastoma brain tumors

Kimball Sheehan¹ · Darrah Sheehan¹ · Mohanad Sulaiman¹ · Frederic Padilla^{2,3} · David Moore² · Jason Sheehan¹ · Zhiyuan Xu¹

Received: 12 March 2020 / Accepted: 17 April 2020 / Published online: 2 May 2020
© Springer Science+Business Media, LLC, part of Springer Nature 2020

Abstract

Objective Glioblastoma is the most common primary brain tumor; survival is typically 12–18 months after diagnosis. We sought to study the effects of sonodynamic therapy (SDT) using 5-Aminolevulinic acid hydrochloride (5-ALA) and high frequency focused ultrasound (FUS) on 2 glioblastoma cell lines.

Procedure Rat C6 and human U87 glioblastoma cells were studied under the following conditions: 1 mM 5-ALA (5-ALA); focused ultrasound (FUS); 5-ALA and focused ultrasound (SDT); control. Studied responses included cell viability using an MTT assay, microscopic changes using phase contract microscopy, apoptotic induction through a caspase-3 assay, and apoptosis staining to quantify cell death.

Results SDT led to a marked decrease in cell extension and reduction in cell size. For C6, the MTT assay showed reductions in cell viability for 5-ALA, FUS, and SDT groups of 5%, 16%, and 47%, respectively compared to control ($p < 0.05$). Caspase 3 induction in C6 cells relative to control showed increases of 109%, 110%, and 278% for 5-ALA, FUS, and SDT groups, respectively ($p < 0.05$). For the C6 cells, caspase 3 staining positivity was 2.1%, 6.7%, 11.2%, and 39.8% for control, 5-ALA, FUS, and SDT groups, respectively. C6 Parp-1 staining positivity was 1.9%, 6.5%, 9.0%, and 37.8% for control, 5-ALA, FUS, and SDT groups, respectively. U87 cells showed similar responses to the treatments.

Conclusions Sonodynamic therapy resulted in appreciable glioblastoma cell death as compared to 5-ALA or FUS alone. The approach couples two already FDA approved techniques in a novel way to treat the most aggressive and malignant of brain tumors. Further study of this promising technique is planned.

Keywords Glioblastoma · Focused ultrasound · Sonodynamic therapy · Apoptosis

Kimball Sheehan and Darrah Sheehan have equal efforts and are co-first authors.

Electronic supplementary material The online version of this article (<https://doi.org/10.1007/s11060-020-03504-w>) contains supplementary material, which is available to authorized users.

✉ Kimball Sheehan
kimballsheehan@gmail.com

¹ Department of Neurological Surgery, Health Sciences Center, University of Virginia, Box 800212, Charlottesville, VA 22908, USA

² Focused Ultrasound Foundation, Charlottesville, VA, USA

³ Department of Radiology, University of Virginia, Charlottesville, VA, USA

Introduction

Glioblastoma represents the most common primary brain tumor, and it is highly aggressive and malignant. There are approximately 200,000 new cases of glioblastoma in the U.S. each year [1]. Glioblastoma patients typically undergo resection followed by radiation therapy and chemotherapy. Despite treatment, glioblastoma patient survival is typically 12–18 months from the time of diagnosis. New treatment options are desperately needed to treat glioblastoma.

The ability to delivered highly FUS to brain targets through the intact skull have become feasible [2]. Such approaches have allowed for the treatment of essential tremor [3]. Other approaches are being explored to use ultrasound to disrupt the blood brain barrier and allow chemotherapy, or novel drug into the brain, mechanical disruption of a tumor, and radiosensitization [4, 5].

The application of FUS with a substance that sensitizes cells to the damaging effects of sound is called SDT [6–11]. It couples ultrasound and a sonosensitizing substance, which are themselves relatively innocuous, but the combination can lead to cell damage and/or death. This sort of approach has great promise for treating cancers that have spread to sensitive areas of the body and, in particular, the brain [12]. Sonodynamic therapy can lead to reactive oxygen species generation and cavitation leading to cell death [12].

Herein, we sought to study the effects of SDT using high frequency, FUS and 5-ALA, a sonosensitizer preferentially taken up by glioblastoma cells [6, 13]. Both are currently approved by the Food and Drug Administration (FDA) and used for other applications in the management of brain tumor patients. We utilize an *in vitro* approach with 2 glioblastoma cells lines to study and optimize SDT. We also sought to quantify the apoptotic potential of SDT in these glioma models.

Methods

Cell lines and cell culture technique

C6 cell line (ATCC CCL-107) are rat glioblastoma cells, and the U87 cell line (ATCC HTB-14) is a human glioblastoma cell line. U87 cells were obtained from ATCC and grown in Eagle's Minimum Essential Medium (ATCC, Manassas, VA, USA) with 10% fetal bovine serum (Hyclone, GE Healthcare Life Sciences) and 1% Gibco antibiotic–antimycotic (Thermo Fisher Scientific, Waltham, Massachusetts, USA). C6 cells were grown in F-12 K medium (ATCC) supplemented with 10% fetal bovine serum (Hyclone) and 1% Gibco antibiotic–antimycotic (Thermo Fisher Scientific, Waltham, Massachusetts, USA).

3-D computer aided design and printing of a platform for focused ultrasound experiments

Using AutoDesk Fusion 360 software and a computer workstation, we designed various mounting devices that would fit a 35 mm dish, 6, 48, and 96 well plates that are commonly used for tissue culture (Supplemental Fig. 1). These devices were printed using a Form 2 resin printer (Form-Labs, Somerville, Massachusetts, USA).

Ultrasound device and optimization of ultrasound treatment parameters

We initially checked a range of power and duty cycles (data not shown) based upon published values [6]. A plane single element FUS transducer (Sonic Concept, Bothell,

WA) was used, 1.1 MHz center frequency and 12 mm diameter. For treatment, the transducer was driven by a function generator (DG1022, Rigol Technologies Inc, Beaverton, OR) connected to a 200 W power amplifier (1020L, E&I, Rochester, NY). To characterize the output of the transducer, pressure measurements were performed using a needle hydrophone (HNA-0400 needle hydrophone, Onda Corp., CA, USA), positioned using computer-controlled 3D positioning mechanical stages. The acoustic signal was acquired with an oscilloscope (DSO7012B, Keysight Technologies) sampling at 100 MHz. The signal was then converted in MPa, after deconvolution from the impulse response for the hydrophone. The spatial distribution of the acoustic field of the transducer was first characterized by measuring the acoustic pressure along the acoustic axis, after propagation through a culture plate. The hydrophone was then positioned at the natural focus of the transducer (maximum pressure), and the acoustic pressure measured for a range of excitation voltage. Assuming a CW plane wave emitted by the transducer, the intensity (I_{SPTA} or Spatial Peak Temporal Average intensity in W/cm^2) was then estimated as $I_{\text{SPTA}} = P^2/(\rho \cdot c)$, where P is the acoustic pressure, ρ (resp. c) is the density (resp. speed of sound) of water.

After initial testing of a range of power and duty cycles (data not shown) based upon published values [6], experiments in which cells were visually inspected after sonication using phase contrast microscopy, the treatment parameters were set to a pressure of P of 500 kPa and a duty cycle of 10%, resulting in an intensity I_{SPTA} of 10 W, delivered over a 3-min period. This treatment regimen did not produce any appreciable temperature rise ($< 1^\circ\text{C}$) nor did it cause overt mechanical damage to the cells.

To estimate possible temperature elevation at the bottom of the culture plate due to absorption of ultrasound energy by the plastic, a thermocouple was used during the power calibration experiments. No appreciable ($< 1^\circ\text{C}$) temperature rise was detected with the selected treatment regimen.

5-Aminolevulinic acid (5-ALA)

5-Aminolevulinic acid hydrochloride (5-ALA; Sigma-Aldrich, St. Louis, Missouri, USA) is an intermediate in heme biosynthesis sonosensitizer that is converted into protoporphyrin IX (PPIX) inside glioma cells. With PPIX excitation at 405 nm or 633 nm, PPIX exhibits fluorescence. Based upon published reports and some experiments evaluating various concentrations of 5-ALA (data not shown), we chose to use a concentration of 1 mM 5-ALA and incubate the cells in 5-ALA for 4 h before initiating experiments [6, 7, 14, 15].

Cell viability assay

Cells grown in 96 well plates were assessed quantitatively for viability using the MTT (3-(4,5-dimethylthiazol-2-yl)-2,5-diphenyltetrazolium bromide) assay (Abcam, Cambridge, MA, USA). The assay relies upon the ability of viable cells with active metabolism to convert MTT into formazan. At the appropriate time, media was carefully aspirated from the wells. Cells were washed with phenol red free DMEM medium to eliminate any effect from the phenol indicator in the medium or the 5-ALA on the colorimetric assay. Next 50 mL of serum and phenol red free DMEM with 10% FBS media and 50 mL of MTT reagent were added to each well. The plate was then incubated at 37 °C for 3 h. After incubation, 150 mL of MTT solvent was added to each well. Cell culture plates were wrapped in aluminum foil and mixed on an orbital shaker for 15 min. Then, absorbance was read at optical density (OD) of 590 nm using a Biotek Synergy HTX plate reader (Winooski, Vermont, USA).

Cell number was computed by relating the OD at 590 nm for a well against a calibration curve constructed with the C6 and U87 cells at concentration ranging from 0 to 100,000 cells per well. Optical density of a test condition was normalized as a ratio of absorbance of the test well versus that of controls run at the same time. MTT assays were run 24 h after treatment with 5-ALA, FUS, SDT, or control conditions with cells initially plated at 30,000 cells/well in 96 well plates. All conditions were run in triplicate with data being expressed as a mean at each condition.

Caspase 3 activity assay

Caspase 3 activity was assessed with a colorimetric caspase 3 assay (Abcam, Cambridge, MA, USA). Cells were washed 2–3 × in phenol free medium to eliminate any effect from the phenol red color or the 5-ALA on the colorimetric assay. Cells were plated at 500,000 cells/well for 96 well plates and at 1,000,000 cells/well for 48 well plates.

The assay was run with a modified protocol based on Abcam's provided instruction by first adding 50 mL of chilled cell lysis buffer and incubating cells on ice for 10 min. Next, we added 50 mL of 2 × reaction assay buffer containing 10 mM DTT was added to each well. An additional 5 mL of 4 mM DEVD-p-NA substrate was added to each well. The cells in the plate were then mixed using an orbital shaker and incubated at 37 °C for 90 min. The absorbance was then read at OD of 400 nm using a Biotek Synergy HTX plate reader (Winooski, Vermont, USA). Optical density was normalized as a ratio of absorbance of the test well versus that of untreated controls run at the same time. All conditions were run in triplicate with data being expressed as a mean at each condition. Caspase 3 assay absorbances were measured 12 to 24 h after treatment with 5-ALA, FUS,

SDT, or control conditions. For control conditions for C6 cells, we checked both a positive control using 0.2 mg/ml of doxorubicin and a negative control (i.e. with no treatment). Doxorubicin (Sigma) at the aforementioned concentration is known to induce apoptosis [16]. The degree of cell apoptosis was computed and expressed relative to control conditions for each cell line. Thus, the degree of apoptosis was expressed as a ratio of the mean absorbance for a particular condition over the mean absorbance of control. As such, a higher ratio of apoptosis for a particular condition means more apoptosis for that treatment versus the control group.

Cytospin preparation and apoptosis staining for caspase-3 and PARP-1

Cells were harvested by trypsinization 24 h after various treatments with 5-ALA, FUS, SDT, or control conditions from 6 well plates (250,000 cells/well at start). Cells were then centrifuged at 1500 rpm for 5 min to pellet them. The tissue culture medium was then aspirated and cells were resuspended in 300 mL of phosphate buffered saline (PBS, Gibco) supplemented with 3% bovine serum albumin (Sigma). Slides and filters were placed into the appropriate slots in a cytospin (StatSpin Cytofuge 2) with the cardboard filters facing the center of the cytospin. 100 mL was aliquoted from each sample into the appropriate wells of the cytospin. The lid of the cytospin is placed over the samples and spun at maximum speed for 3 min. The filters were then removed from the slides without contacting the smears on the slides. The slides were examined under a microscope to confirm normal morphology of the cells. The slides were then placed in a desiccation chamber for approximately 2 h and kept in –80 °C until immunohistochemistry was performed.

Next, immunohistochemistry was performed using a robotic platform (Ventana discover Ultra Staining Module, Ventana Co., Tucson, AZ, USA). Initially, slides were dried at room temperature for 2 h; then they were fixed with equal volumes of chilled acetone and ethanol for 10 min at 4 °C. Endogenous peroxidases were blocked with peroxidase inhibitor for ~8 min before incubating the specimens with cleaved caspase 3 (Cell signaling, Cat#9661) and anti-cleaved PARP-1 (Abcam, Cat #ab 32,064) antibodies at 1:100 and 1:200 dilution, respectively, for 60 min at ambient temperature. Antigen–antibody complex was then detected using OmniMap anti-rabbit multimer RUO detection system (ChromoMap DAB Kit, Ventana Co.). All the slides were counterstained with hematoxylin subsequently. Then, they were dehydrated and mounted for assessment.

Using a Nikon inverted microscope at 20 × and 40 ×, 5 randomly selected fields of view, were manually counted for caspase 3 or PARP-1 positive staining cells on each slide for a particular given condition.

Cell morphological changes

Using phase contrast microscopy on a Nikon or Zeiss inverted microscope to view the cells under a given condition, cells were assessed for distinct morphological changes associated with apoptosis including shrinkage of the cell, detachment of the cell from surrounding cells, condensation of the nuclear chromatin, and retraction or elimination of cellular extensions of the glioma cells [17].

Data and statistical analysis

Experimental conditions was performed in triplicate, and mean and standard error of the mean were computed for each experimental condition and time point. Groups were statistically compared to one another with a *t* test (IBM Corporation, SPSS Statistics for Windows, version 24. Armonk, NY and Excel, Microsoft). A *p* value < 0.05 was considered statistically significant.

Results

Cell uptake of 5-ALA

After loading with 1 mM 5-ALA, under phenol free medium, both C6 and U87 cells showed a bright fluorescence typical of conversion of 5-ALA to protoporphyrin IX (i.e. the fluorescent byproduct of 5-ALA) with fluorescence as shown in Fig. 1a, b.

Cell morphological changes

U87 and C6 cells exhibited normal cellular processes when grown in culture medium. When exposed to 5-ALA, the cells were able to convert it to PPIX wherein they exhibited fluorescence. However, the morphology of the cells did not appreciably change when cells were incubated with 5-ALA or treated with ultrasound alone. When treated with SDT, the cells showed a more rounded appearance as well as a combined retraction (i.e. shrinkage) and general reduction in the number of cellular extensions (Fig. 1c, d).

Cell viability changes with MTT assay

The calibration curves for cell viability as assessed by the MTT assay were performed. Within the range from 0 to 100,000 cells/well in the 96 well plates, the U87 and C6 cells demonstrated a fairly linear relationship between cell number and absorbance (Fig. 2a, b).

MTT cell viability assay results were computed and expressed relative to untreated control conditions for each cell line. For C6, the MTT assay showed reductions in cell

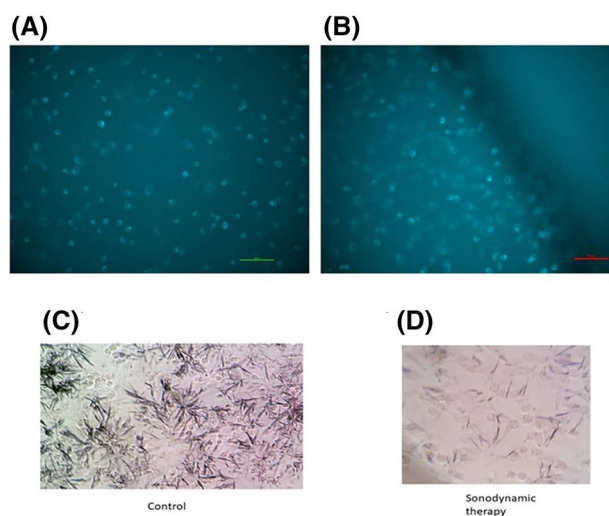


Fig. 1 These micrographs demonstrating fluorescence of U87 cells after exposure to 1 mM 5-ALA for 4 h with magnification at 100× (a green scan bar 50 microns) and 200× (b red scale bar 100 microns) excitation at 405 nm and high pass filter of 625 nm. Phase contrast light microscopy views of control c and sonodynamic therapy, d treated C6 wells approximately 24 h after treatment with 1 mM 5-ALA and 10 W/cm² ultrasound (100× magnification)

viability for 1 mM 5-ALA, 10 W/cm² FUS, and SDT (i.e. combined 1 mM 5-ALA and 10 W/cm² FUS) groups of 5%, 16%, and 47%, respectively compared to control (*p* = 0.005 comparing SDT and FUS group) (Fig. 3a, b). For U87 cells, the MTT assay reductions in viability for 5-ALA, FUS, and SDT groups were 6%, 27%, and 46%, respectively compared to the control group (*p* = 0.001 comparing SDT and FUS group).

Apoptosis induction via caspase 3 assay

Caspase 3 activity in cells was measured under test conditions of 5-ALA, FUS, and SDT for C6 and U87 glioblastoma cells.

For C6 cells, the caspase 3 assay showed increased expression of 222%, 109%, 110%, and 279% for doxorubicine positive control, 5-ALA (1 mM), FUS (10 W/cm²), and SDT groups, respectively compared to the negative (i.e. untreated) control group (*p* < 0.001 comparing SDT to FUS) (Fig. 3c, d). For the U87 cells, the caspase 3 assay showed increased expressions for 5-ALA, FUS, and SDT groups of 118%, 120%, and 137%, respectively compared to the control group (*p* < 0.001 comparing SDT to FUS).

Apoptosis staining for caspase 3

Apoptosis immunohistochemical staining of C6 and U87 cells was performed to cross-validate the findings of the above caspase 3 assay. In the control setting, caspase 3

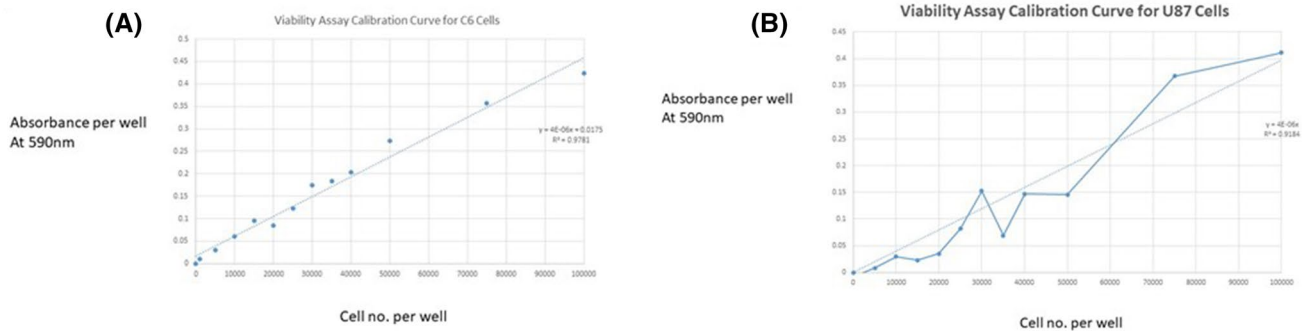


Fig. 2 MTT Calibration curves for **a** C6 and **b** U87 cells over the range of 0–100,000 cells per well of a 96 well plate measured at an absorbance of 590 nm light

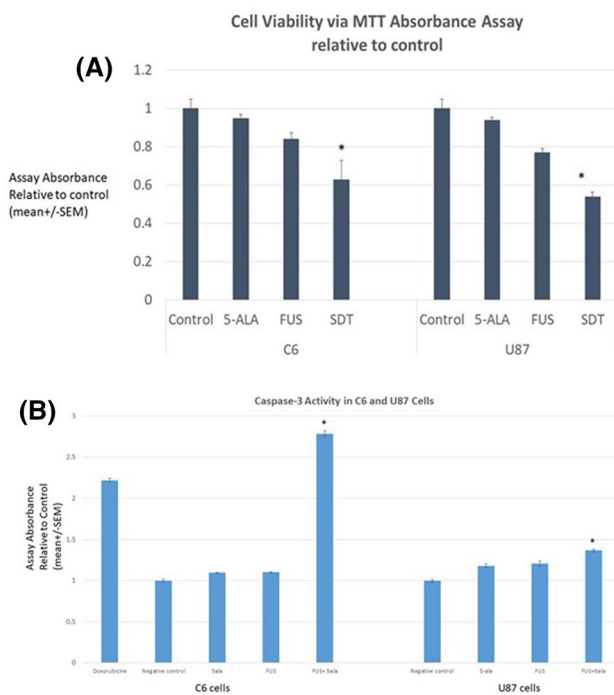


Fig. 3 Cell viability assessed with MTT Assay C6 (**a**) and U87 (**b**) cells for control, 1 mM 5-ALA, 10 W/cm² FUS, and Sonodynamic therapy (i.e. FUS and 5-ALA) conditions. Data are shown as mean \pm standard error of the mean and are normalized to the control condition. *denotes $p < 0.05$ relative to FUS, 5-ALA, and control groups. Apoptosis assessed with caspase 3 Assay C6 (**c**) and U87 (**d**) cells for control (negative, untreated control and positive control with doxorubicine), 1 mM 5-ALA, 10 W/cm² FUS, and Sonodynamic therapy (i.e. FUS and 5-ALA) conditions. Data are shown as mean \pm standard error of the mean and are normalized to the control condition. *denotes $p < 0.05$ relative to FUS, 5-ALA, and negative control groups

immunohistochemical staining was positive in $2.1 \pm 0.3\%$ of C6 cells and $1.5 \pm 0.18\%$ of U87 cells, (Fig. 4a, b). Incubation with 5-ALA (1 mM for 4 h) resulted in an increase in caspase 3 staining, with $6.8 \pm 0.2\%$ positive C6 cells and $5.2 \pm 0.51\%$ positive U87 cells. Ultrasound treatment alone

led to mean positive staining in the C6 and U87 cells of $11.2 \pm 0.24\%$ and $9.6 \pm 0.48\%$, respectively. The SDT group (US and 5-ALA) had mean positive caspase staining for C6 and U87 cells of $39.8 \pm 0.45\%$ and $38.1 \pm 0.67\%$, respectively ($p < 0.05$ compared to control, FUS, and 5-ALA groups for both C6 and U87 cells).

Apoptosis staining for parp-1

Parp-1 expression occurs downstream of caspase 3 in the apoptotic cascade, and it serves to promote apoptosis by inhibiting DNA repair induced survival of cells [18]. In the control setting, the mean (\pm SEM) Parp-1 staining percentages of C6 and U87 cells positivity were $1.9 \pm 0.25\%$ and $2.1 \pm 0.32\%$, respectively (Fig. 5a, b). For C6 cells, the percentages of PARP-1 staining for 5-ALA, FUS, and SDT treated groups, 24 hr post-treatment, were $6.5 \pm 0.4\%$, $9 \pm 0.45\%$, and $37 \pm 1.2\%$, respectively. For U87 cells, the percentages of PARP-1 staining for 5-ALA, FUS, and SDT treated cells were $6 \pm 0.6\%$, $8.4 \pm 0.3\%$, and $39.7 \pm 1.16\%$, respectively. The PARP-1 staining for the SDT treated groups was statistically significantly increased over the other groups ($p < 0.01$ for both C6 and U87 cells).

Discussion

In his book entitled *The Tumor*, Grisham predicted a future in which ultrasound could be used to treat patients harboring a glioblastoma [19]; this might include ultrasound for thermal ablation but also the use of focused ultrasound for SDT. Glioblastomas represent the most malignant of brain tumors. Even with standard of care treatments, average survival for a glioblastoma patients is only 12–18 months after diagnosis [1]. Sonodynamic therapy combines a sonosensitizer with FUS to effect a change within targeted cells. SDT is used to treat cancer and effect cellular damage or death of the tumor cells. One mechanism of cellular damage or death arising

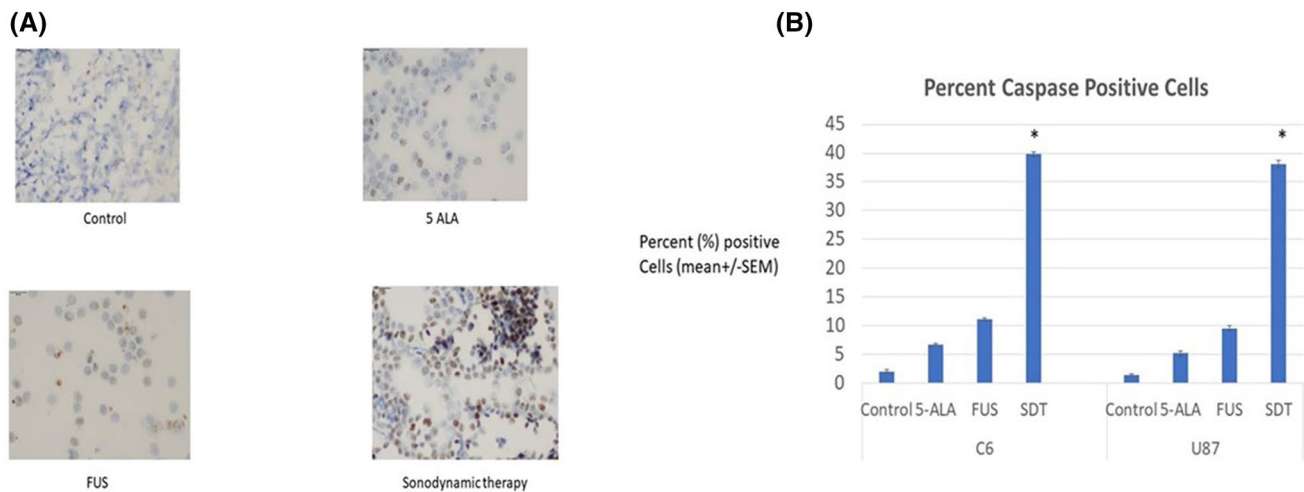


Fig. 4 **a** Caspase Staining of C6 glioma cells for control, 1 mM 5-ALA, 10 W/cm² FUS, and Sonodynamic therapy (i.e. FUS and 5-ALA) conditions (40×magnification). **b** Percentage of caspase positive cells for C6 and U87 cells for control, 1 mM 5-ALA, 10 W/cm² FUS, and Sonodynamic therapy (i.e. FUS and 5-ALA) conditions. Data are shown as mean ± standard error of the mean. *denotes p < 0.05 relative to FUS group

cm² FUS, and Sonodynamic therapy (i.e. FUS and 5-ALA) conditions. Data are shown as mean ± standard error of the mean. *denotes p < 0.05 relative to FUS group

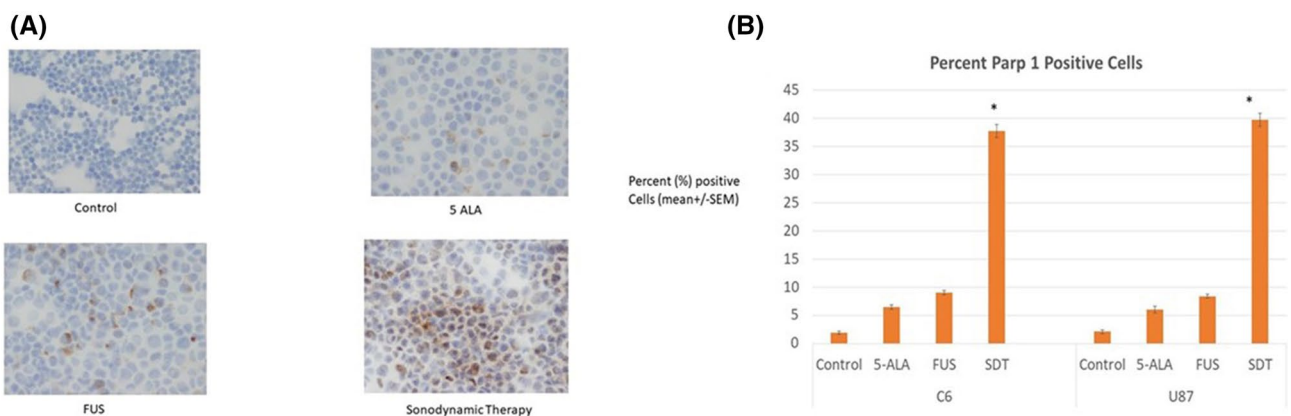


Fig. 5 **a** Parp-1 Staining of C6 glioma cells for control, 1 mM 5-ALA, 10 W/cm² FUS, and Sonodynamic therapy (i.e. FUS and 5-ALA) conditions (40×magnification). **b** Percentage of Parp-1 positive cells for C6 and U87 cells for control, 1 mM 5-ALA, 10 W/cm² FUS, and Sonodynamic therapy (i.e. FUS and 5-ALA) conditions. Data are shown as mean ± standard error of the mean. *denotes p < 0.05 relative to FUS group

cm² FUS, and Sonodynamic therapy (i.e. FUS and 5-ALA) conditions. Data are shown as mean ± standard error of the mean. *denotes p < 0.05 relative to FUS group

from SDT is the generation of reactive oxygen species and cavitating bubbles. Such reactive oxygen species and bubbles can damage the tumor cell's DNA, RNA, proteins, and lipids leading to apoptosis.

To study the effects of SDT, we first designed and constructed devices to couple the FUS to commonly utilized tissue culture dishes. The 3-D engineered devices were specifically fit to the ultrasound transducer and tissue culture plates or dishes used. They were also immersible and stable in water. The water tank in which the experiments were conducted served to minimize the defocusing of the ultrasound that would occur in an environment in which gas was situated between the probe and the cell.

Next studying glioblastoma cells, we treated them with 5-ALA, FUS, or SDT. We observed a decrease in cell viability, change in morphology, and an increase in apoptotic cell death activation with the treatment of 5-ALA or FUS. When the 5-ALA and FUS were combined, the effects in terms of diminished cell viability and activation of apoptosis were appreciably increased. We choose to cross-validate our findings by using both commercially available colorimetric assays and immunohistochemical staining for apoptotic cell death. The trends in the assays were consistent with those observed with semi-quantitative cell counting assessments derived from standard immunohistochemical staining tests.

Given that 5-ALA is preferentially taken up in glioma cells and that ultrasound can be aimed and focused with MRI guidance, SDT has potential use for treating patients with gliomas [13, 20]. The current study demonstrates the ability of two relatively innocuous agents—FUS and 5-ALA—to impact the viability of malignant glioma cells. 5-ALA is converted to PPIX and predominantly located in mitochondria where it can generate reactive oxygen species and lead to apoptosis. In another recent study using *in vivo* and *in vitro* glioma models, Yoshida et al. [21] demonstrated the ability of SDT using 18 W ultrasound power and 200 mg/mL 5-ALA to reduce F98 cell viability through reduction in cell proliferation, invasiveness, and induction of apoptosis [21]. In another study of SDT for human oral squamous cell carcinoma, treatment with SDT resulted in an increase in apoptosis of 3 × and 14 × that of the ultrasound and control groups, respectively [22]. SDT has also been shown to be effective in inducing an anti-tumor response when coupled with immunotherapies such as Opdivo and Keytruda using models such as mice bearing 4T1 subcutaneous tumors and murine colorectal cancer models [23]. Our current study findings are in keeping with prior studies that show an appropriate sonosensitizer and FUS can induce non-thermal damage and/or death to cancer cells superior to what either agent could accomplish; our work represents a comprehensive assessment of the apoptotic potential of SDT using semi-quantitative and quantitative assessments of both rat and human derived glioma cells. Beyond its role as a sonosensitizer, 5-ALA has also been considered as a radiosensitizer.

The current research serves an approach to study and optimize sonodynamic parameters and test various sonosensitizers for primary brain tumor types. It can also be used to study other types of tumors including lung cancer, breast cancer, and melanoma which frequently metastasize to the brain. The current set-up allows for exploration of different FUS frequencies, powers, and duty cycles. It also allows for the study of other types and concentrations of sonosensitizers. The experimental data can be used to pursue preclinical testing using brain tumor animal models and also eventually testing in the form of a clinical trial.

Sonodynamic therapy can also be easily integrated into the current standard of care for many types of cancers including glioblastoma [24]. Because of its relatively innocuous agents, SDT is easily combined with other types of adjuvant therapies such as radiation therapy, photodynamic therapy, chemotherapy, and gene therapy. Studies have shown that SDT can enhance the sensitivity of cancer cells to chemotherapeutic drugs and radiation therapy [25]. For example, in a study by Wang et al., they found that the combination of doxorubicin in combination with PpIX and low intensity ultrasound led to significantly more cell death than with either the drug or the SDT alone [26]. As such, the

therapeutic advantages of SDT may go well beyond itself, and the SDT approach could be integrated into other adjuvant therapies.

The study is not without limitations. We explored only two glioblastoma cell lines. While these cell lines are commonly used in research, other cell lines may behave differently under the same experimental conditions. Thus, there is a need to study additional glioma cell lines in future studies. However, the platform developed herein will allow us to do so in the future. Cytoskeleton changes within the cells warrant further investigation as part of the morphologic changes seen in this research. Also, apoptosis and the generation of reactive oxygen species can also be studied with flow cytometry; while not performed herein, we are actively expanding our work to incorporate these techniques for future studies. Also, the FUS was a single emitter, and multiple emitters would likely be used for clinical purposes. It is possible that with an array of multiple FUS emitters, the power of the FUS can be more evenly distributed across a larger treatment area. To penetrate the human skull, it is likely that more than one FUS emitter will be needed to adequately deliver ultrasound to a brain tumor. However, such devices do currently exist and include the Exablate 4000 system (Insightec, Tirat Carmel, Israel).

Conclusions

5-ALA is readily taken up and converted to protoporphyrin IX in C6 and U87 glioblastoma cells. 5-ALA alone and FUS alone resulted in no appreciable glioblastoma cellular damage, but SDT resulted in appreciable apoptosis mediated cellular damage to various malignant glioblastoma cells. We have developed a platform that can be used for rapid and high throughput screening of cell types and sonosensitizers, and it can be used to optimize treatment settings before pre-clinical or clinical testing. Further *in vitro* testing and optimization of ultrasound and sonosensitizers can be performed with our experimental glioma models. FUS and sonosensitizers have substantial potential for treatment of malignant brain tumors and other challenging oncology indications.

Acknowledgements We are grateful for the support of Drs. Eames and Moore who allowed us to use their 3D CAD software and 3D printer at the Focused Ultrasound Foundation. Finally, we appreciate the assistance of Dr. Pramoonjago at the University of Virginia's Biorepository and Tissue Research Facility who processed the cells using automated instrumentation for the cytospin techniques for immunohistochemical staining.

Compliance with ethical standards

Ethical approval The current research does not involve human participants and/or animals and therefore informed consent was not required.

Disclosures Dr. Padilla and Dr. Moore are employees of the Focused Ultrasound Foundation. Otherwise, the authors have no disclosures related to this particular study.

References

- Omuro A, DeAngelis LM (2013) Glioblastoma and other malignant gliomas: a clinical review. *JAMA* 310(17):1842–1850
- McDannold N, Clement GT, Black P, Jolesz F, Hynynen K (2010) Transcranial magnetic resonance imaging—guided focused ultrasound surgery of brain tumors: initial findings in 3 patients. *Neurosurgery* 66(2):323–332
- Walters H, Shah BB (2019) Focused ultrasound and other lesioning therapies in movement disorders. *Curr Neurol Neurosci Rep* 19(9):66
- Fishman PS, Frenkel V (2017) Focused ultrasound: an emerging therapeutic modality for neurologic disease. *Neurotherapeutics* 14(2):393–404
- Zhu L, Altman MB, Laszlo A et al (2019) Ultrasound hyperthermia technology for radiosensitization. *Ultrasound Med Biol* 45(5):1025–1043
- McHale AP, Callan JF, Nomikou N, Fowley C, Callan B (2016) Sonodynamic therapy: concept, mechanism and application to cancer treatment. *Adv Exp Med Biol* 880:429–450
- Yang Y, Tu J, Yang D, Raymond JL, Roy RA, Zhang D (2019) Photo- and sono-dynamic therapy: a review of mechanisms and considerations for pharmacological agents used in therapy incorporating light and sound. *Curr Pharm Des* 25(4):401–412
- Endo S, Kudo N, Yamaguchi S, Sumiyoshi K, Motegi H, Kobayashi H, Terasaka S, Houkin K (2015) Porphyrin derivatives-mediated sonodynamic therapy for malignant gliomas in vitro. *Ultrasound Med Biol* 41(9):2458–2465
- Jeong EJ, Seo SJ, Ahn YJ, Choi KH, Kim KH, Kim JK (2012) Sonodynamically induced antitumor effects of 5-Aminolevulinic acid and fractionated ultrasound irradiation in an orthotopic rat glioma model. *Ultrasound Med Biol* 38(12):2143–2150
- Lafond M, Yoshizawa S, Umemura SI (2019) Sonodynamic therapy: advances and challenges in clinical translation. *J Ultrasound Med* 38(3):567–580
- Pan X, Wang H, Wang S, Sun X, Wang L, Wang W, Shen H, Liu H (2018) Sonodynamic therapy (SDT): a novel strategy for cancer nanotheranostics. *Sci China Lif Sci* 61(4):415–429
- Hersh DS, Kim AJ, Winkles JA, Eisenberg HM, Woodworth GF, Frenkel V (2016) Emerging applications of therapeutic ultrasound in neuro-oncology: moving beyond tumor ablation. *Neurosurgery* 79(5):643–654
- Hadjipanayis CG, Widhalm G, Stummer W (2015) What is the surgical benefit of utilizing 5-Aminolevulinic acid for fluorescence-guided surgery of malignant gliomas? *Neurosurgery* 77(5):663–673
- Li YJ, Huang P, Jiang CL, de Jia X, Du XX, Zhou JH, Han Y, Sui H, Wei XL, Liu L, Yuan HH, Zhang TT, Zhang WJ, Xie R, Lang XH, Wang LY, Liu T, Bai YX, Tian Y (2014) Sonodynamically induced anti-tumor effect of 5-Aminolevulinic acid on pancreatic cancer cells. *Ultrasound Med Biol* 40(11):2671–2679
- Li Y, Zhou Q, Hu Z, Yang B, Li Q, Wang J, Zheng J, Cao W (2015) 5-Aminolevulinic acid-based sonodynamic therapy induces the apoptosis of osteosarcoma in mice. *PLoS ONE* 10(7):e0132074
- Ji C, Yang B, Yang YL, He SH, Miao DS, He L, Bi ZG (2010) Exogenous cell-permeable C6 ceramide sensitizes multiple cancer cell lines to Doxorubicin-induced apoptosis by promoting AMPK activation and mTORC1 inhibition. *Oncogene* 29(50):6557–6568
- Saraste A, Pulkki K (2000) Morphologic and biochemical hallmark of Apoptosis. *Cardiovasc Res* 45(3):528–537
- D'Amours D, Sallmann FR, Dixit VM, Poirier GG (2001) Gain-of-function of poly(ADP-ribose) polymerase-1 upon cleavage by apoptotic proteases: implications for apoptosis. *J Cell Sci* 114(20):3771–3778
- Grisham J (2015) *The Tumor*. eBook.
- Fomenko A, Lozano AM (2019) Neuromodulation and ablation with focused ultrasound—toward the future of noninvasive brain therapy. *Neural Regen Res* 14(9):1509–1510
- Yoshida M, Kobayashi H, Terasaka S, Endo S, Yamaguchi S, Motegi H, Itay R, Suzuki S, Brokman O, Shapira Y, Moriyama K, Kawase Y, Akahane T, Kato Y, Kamada H, Houkin K (2019) Sonodynamic therapy for malignant glioma using 220-kHz transcranial magnetic resonance imaging-guided focused ultrasound and 5-Aminolevulinic acid. *Ultrasound Med Biol* 45(2):526–538
- Lv Y, Zheng J, Zhou Q, Jia L, Wang C, Liu N, Zhao H, Ji H, Li B, Cao W (2017) Antiproliferative and apoptosis-inducing effect of exo-protoporphyrin IX based sonodynamic therapy on human oral squamous cell carcinoma. *Sci Rep* 7:40967
- Yue W, Chen L, Yu L, Zhou B, Yin H, Ren W, Liu C, Guo L, Zhang Y, Sun L, Zhang K, Xu H, Chen Y (2019) Checkpoint blockade and nanosonosensitizer-augmented noninvasive sonodynamic therapy combination reduces tumour growth and metastases in mice. *Nat Commun* 10(1):2025
- Wan GY, Liu Y, Chen BW, Liu YY, Wang YS, Zhang N (2016) Recent advances of sonodynamic therapy in cancer treatment. *Cancer Biol Med* 13(3):325–338
- Wang X, Jia Y, Wang P, Liu Q, Zheng H (2017) Current status and future perspectives of sonodynamic therapy in glioma treatment. *Ultrason Sonochem* 37:592–599
- Wang X, Jia Y, Su X, Wang X, Zhang K, Feng X et al (2015) Combination of protoporphyrin IX-mediated sonodynamic treatment with doxorubicin synergistically induced apoptotic cell death of a multidrug-resistant leukemia K562/DOX cell line. *Ultrasound Med Biol* 41:2731–2739

Publisher's Note Springer Nature remains neutral with regard to jurisdictional claims in published maps and institutional affiliations.